MICRO-SCRATCH FOR COATING ADHESION TEST OF NANO-STRUCTURED TiB_2 COATINGS

Nurot Panich*, Naing Naing Aung and Sun Yong

Received: Jan 17, 2005; Revised: Apr 20, 2005; Accepted: Apr 25, 2005

Abstract

TiB_2-based nano-structured coatings were fabricated on high-speed steel by magnetron sputtering technique. Mechanical characterization of the resultant coating-substrate systems, such as, coating adhesion, friction and scratch resistance, was conducted by micro-scratch techniques. The linearly-increasing load mode of the micro-scratch tests was studied to determine the most effective and informative testing conditions and to determine the critical load (Lc) for coating failure. The mode of failure was examined by high resolution SEM and AFM. By applying a small substrate bias and controlling the sputter-cleaning time, it was found the coating adhesion strength with high hardness was significantly improved.

Keywords: Micro-scratch, nanoindentation, titanium diboride coating, adhesion, hardness, critical load

Introduction

Titanium diboride, TiB_2, is well known as a ceramic material with a hexagonal structure, which presents various attractive properties, such as high hardness and excellent corrosion, thermal oxidation and wear resistance (Cutler, 1991; Munro, 2000). TiB_2 coatings are easy to deposit by various approaches; one of the most commonly used is magnetron sputtering due to the low cost of operation. Although many attempts have been made to utilize this material as a protective coating, its real and commercial applications have been very limited owing to the difficulties in producing TiB_2 coatings with good mechanical integrity (Berger *et al.,* 2004).

The major problem in producing high quality TiB_2 coatings is that the adhesion of a TiB_2 coating is poor for the coating-substrate system. Actually, the adhesion of the coating is the most critical aspect of the coating-substrate system particularly for tribological applications. Recently, Berger *et al*. (2001) developed a method to fabricate TiB_2 coatings by d.c. magnetron sputtering by applying a positive substrate bias which could improve the adhesive strength without deteriorating the coating hardness, while this could not be done by using a negative substrate bias. On the other hand, Panich and Sun (2005) addressed how the deposition process can be controlled to produce a TiB_2 coating with both high hardness and good

School of Materials Science and Engineering, Nanyang Technological University, Singapore 639798.
E-mail: panich@pmail.ntu.edu.sg
** Corresponding author*

adhesion strength. This is achieved by introducing substrate sputter-cleaning and then biasing (rf negative) for the early stage of deposition, followed by deposition without biasing.

In order to determine and analyze the adhesion strength of a coating or thin film to a substrate, a scratch test is widely used by research laboratories as well as the industry. In the present work, attempts were made to enhance the adhesion of TiB_2-based nano-structured coatings onto high-speed steel substrates with high coating hardness, by applying a small substrate bias and controlling the sputter-cleaning time. This paper discusses further the effect of sputter-cleaning time, with respect to hardness and scratch resistance of the resultant coatings.

Materials and Methods

Sample Pretreatment

High-speed steel, (HSS, SECO WKE45, Sweden) was chosen as a substrate in this study. HSS was cut into 12 mm × 12 mm × 3 mm pieces. A specimen's surface was prepared by grinding and polishing and was then ultrasonically cleaned for 10 min before charging into the deposition chamber.

Experimental Procedure

High-purity argon gas was introduced into the deposition chamber after it was evacuated to below 5×10^{-4} Pa. The Ti target was powered in the direct current (dc) mode and the TiB_2 target was powered in the radio frequency (rf) mode. In order to clean up the targets, they were pre-sputtered for 10 min with the target shutters closed. The working table on which specimens were placed was rotating at 6 rpm during the process. The substrate to target distance was held constant at 10 cm for the dc target (Ti) and at 5 cm for the rf target (TiB_2). All the experiments were conducted at a constant working pressure of 0.65 Pa and at a total Ar flow rate of 20 sccm (standard cubic centimeter). The substrate temperature was 400°C for all depositions. A rf power biased to the substrate was used before deposition in order to sputter-clean the substrate surface by using a power of 150 W and a rf power of 30 W was also provided to the substrate as bias during the first hour of deposition. The remaining two hours of deposition were conducted without substrate bias. A thin pure Ti interlayer (about 50 nm) was deposited first, by sputtering the Ti target for 10 min with a dc power of 200 W. This was followed by sputtering of the TiB_2 target for 3 h with a rf power of 200 W. Process variation was studied with reference to the effect of sputter-cleaning of the substrate before deposition as summarised in Table 1 and the deposition set up is schematically shown in Figure 1.

The nanoindentation test was performed using the NanoTest™ (Micro Materials Limited, UK), with a Berkovich diamond indenter. All experiments were performed at a constant loading and unloading rate of 0.1 mN/s and to a maximum penetration depth of 50 nm (in order to avoid the effect of the substrate). The unloading curves were used to derive the hardness and reduced modulus values by the analytical technique developed by Oliver and Pharr (1992).

Coating thickness was examined by ball crater (Calotest, Switzerland). A stainless steel ball of 24.5 mm diameter was used for cratering with speed of 500 rpm for 240 s. The scratch tracks were investigated by scanning electron microscope (SEM) (Joel 5410). Atomic force

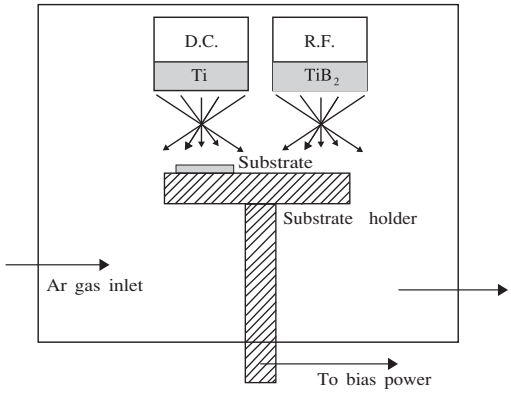

Figure 1. The deposition set up in this study

microscopy (AFM), Digital Instrument, Santa Barbara, CA, was used to investigate the scratch track of the resultant coatings tested by micro-scratch test.

The micro-scratch test was performed using the multipass wear test mode available in the NanoTest™ device with an indenter topped with a conical spherical end form of 25 mm in radius. The stylus was moved tangential to the surface at a speed of 25 mm/s over a length of 1,000 mm. After an initial 300 mm pre-scan under a small load of 0.25 mN, a testing load was applied to the indenter with the linearly increasing load of 25 mN/s. For each scratch test, a set of surface profiles along the track was measured i.e. the track profile before scratch (BS) by measuring the surface profile (surface topography) across the full length of the measured distance (1,000 mm) with the small load of 0.25 mN, and during scratch (DS) by measuring the surface profile after the BS step with the increasing load after the pre-scan length (Xia *et al.,* 2004). The critical load for coating failure (Lc), a coefficient of friction and variation of properties with depth can be determined under a micro-scratch test. The method to determine the Lc is a test that consists of applying a continuously increasing load on the coating surface by a stylus whilst the sample is moved at a constant speed. The stylus causes increasing elastic and plastic deformation until damage takes place in the surface region. In practice, the film may not be removed entirely from the channel so it is convenient to address a Lc which characterises the mechanical adhesion strength of the coating/substrate systems

Results and Discussion

Nanoindentation Test

There has been a wide range of hardness and modulus values reported for TiB_2-based coatings produced under different conditions. It is well known that for real application of hard coatings, the hardness required is around 20 - 40 GPa and can be achieved in TiB_2 coatings. It is not necessary to produce coatings that are too hard, and the adhesion strength, which is the subject of this work, must also be seriously considered. In order to assess the intrinsic mechanical properties of the coatings, all specimens were tested at 50 nm penetration depths to minimise the effect the of substrate. The reported hardness and modulus values are the average of 10 measurements. Figure 2 shows the typical load-displacement curves of samples 3 and 5 (in order to study the benefit of sputter-cleaning time). The hardness and modulus values as measured by nanoindentation are summarised in Table 1.

It can be seen that samples 2 - 5 produced with a substrate bias of 30 W for the first hour only have relatively low hardness and modulus (Table 1), compared with that produced without biasing (sample 1). Indeed, substrate biasing

Table 1. Summary of deposition conditions and properties of studied samples

Materials	Sputter - cleaning of substrate	Substrate bias (w)	Coating thickness (nm)	Hardness (GPa)	Reduced modulus (GPa)	Critical load Lc (mN)
Sample 1	No sputter-cleaning	No bias	700	28.4 ± 1.2	307.2 ± 8.2	353.7
Sample 2	No sputter-cleaning	30 W for the first hour only	650	19.2 ± 1.7	235.5 ± 6.4	529.1
Sample 3	rf 150 W 30 min	30 W for the first hour only	650	20.8 ± 0.9	242.5 ± 11.2	595.4
Sample 4	rf 150 W 60 min	30 W for the first hour only	600	23.6 ± 1.9	275.1 ± 8.5	648.5
Sample 5	rf 150 W 90 min	30 W for the first hour only	550	26.4 ± 1.5	283.2 ± 9.6	875.5

during deposition causes a drop in coating hardness and modulus. However, substrate cleaning helps to improve the hardness and modulus. With increasing sputter-cleaning time, the hardness and modulus increase significantly as shown in Figure 3(a). As confirmed by load-displacement curves (Figure 2), at shorter sputter-cleaning time (sample 3) the coating experiences significant plastic deformation, which can be observed during unloading stage of (sample 3), but the coating produced with longer sputter-cleaning time experiences significant elastic recovery during the unloading stage (sample 5 in Figure 2), possesses a much higher hardness of around 26.4 GPa and a higher modulus of 283.2 GPa, as well as better coating-substrate adhesion (Figure 3(b)), as discussed below.

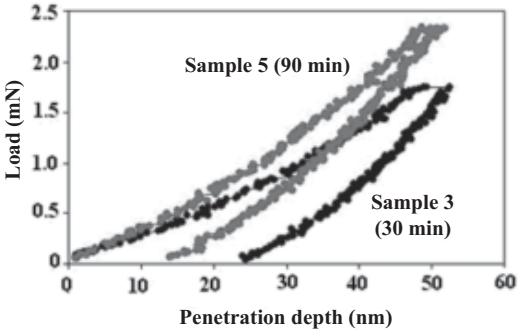

Figure 2. Load-displacement curves of samples 3 and 5 extracted at the penetration depth of 50 nm

From this result, it is obvious that the benefit of substrate sputter cleaning is to enhance the mechanical properties of the coating systems. In order to understand the reason for the improvement of the coating properties, the mechanism of substrate-cleaning was investigated. In substrate sputter (plasma) cleaning, the specimen is sputtered by Ar ions before deposition process. The process of plasma substrate-cleaning is given in Figure 4. This process and mechanism are as same as target sputtering cleaning. In addition, the time required for cleaning the substrate to eliminate all oxides or contaminant layers at the top surface should be appropriate and should be long enough for the Ar ions to interact by etching onto the clean surface of the substrate. It is well known that the oxide or contaminant layers weaken the coating adhesion. By reducing the oxide or contaminant layers, it is believed that the coating adhesion and mechanical properties could be improved due to the enhanced film quality.

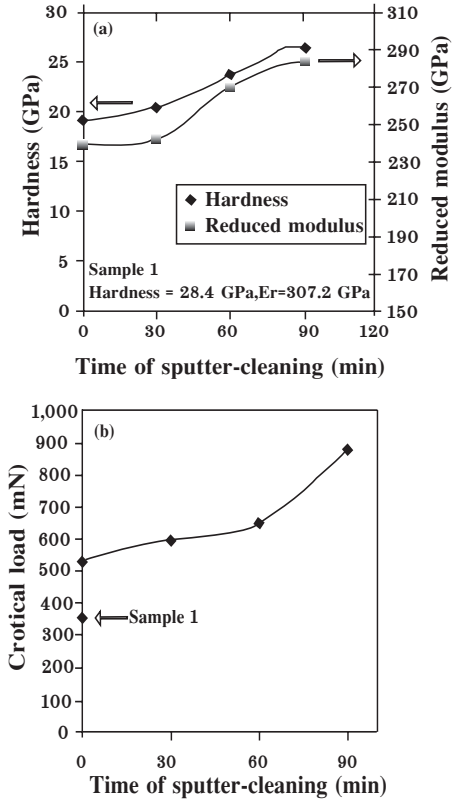

Figure 3. The effect of sputter-cleaning time on (a) hardness and reduced modulus, and (b) critical load

Micro-scratch Test

From Figure 3 (b), it is obvious that with increasing sputter-cleaning time, the critical load for coating adhesion failure (Lc) increases significantly. For instance, the Lc of sample 5 increases by almost 3 times that of sample 1 (no sputter-cleaning and no substrate bias). It indicates that substrate cleaning helps to improve the critical load or coating adhesion strength. Figure 5 shows the typical scratch

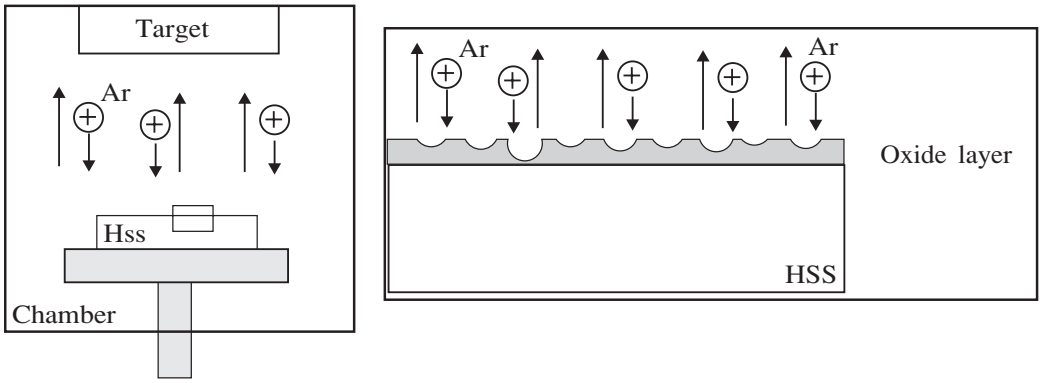

Figure 4. Mechanism of plasma substrate cleaning

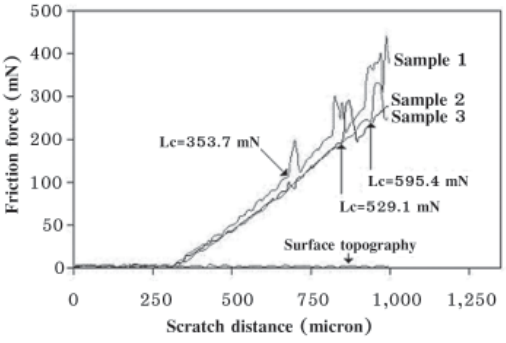

Figure 5. Micro-scratch curves of deposited TiB_2 coatings under linearly-in creasing load

curves with a linearly-increasing load for the TiB_2 coatings. It can be seen that the surface topography measured at the BS step has the same profile for all tests.

It is obvious that after an initial 300 mm pre-scan, all DS profiles increase almost linearly with an increasing load until a certain point. The large fluctuations in the profiles indicate the damage of the TiB_2 coating, as further confirmed by SEM image (Figure 6). Therefore, the scratch load at this point can be taken as the critical load (Lc) for coating failure. The Lc values for all coatings are also listed in Table 1. This phenomenon was further verified by SEM examination of the resultant scratches to identify the scratch mode of failure of coatings as shown in Figure 6.

SEM examination revealed that coating failure of sample 1, produced without sputter-cleaning and bias, is typical of the compressive spallation failure mode (Figure 6(a)). However, after introducing substrate bias resulted in the reduction of the hardness and modulus, the coating adhesion is improved which can be seen from the increase of critical load value. It is also noted that the failure mode has been changed from compressive spallation to wedge spallation (Figure 6(b)), which obviously shows the improvement of the coating adhesion strength. The wedge spallation occurs because of the accumulation of residual stress during the stylus motion. Wedge spallation occurs instead of compressive spallation because the coating adhesion is strong enough to bear the stress. In addition, compressive shear crack is formed in the coating leading to interfacial detachment (Figure 6(b)).

Figure 6(c) shows the failure mode of sample 3 produced with sputter-cleaning for 30 min and a substrate bias of 30 W for the first hour. The failure mode also is the wedge spallation with a smaller damaged area or less wearing out of the coating. It is shown that with sputter-cleaning, the coating adhesion strength is increased. When the sputter-cleaning time is longer, the wedge spallation mode is changed to micro-cutting (no coating failure) (Figure 6(d)), which occurs due to the physical interaction between the stylus and the surface

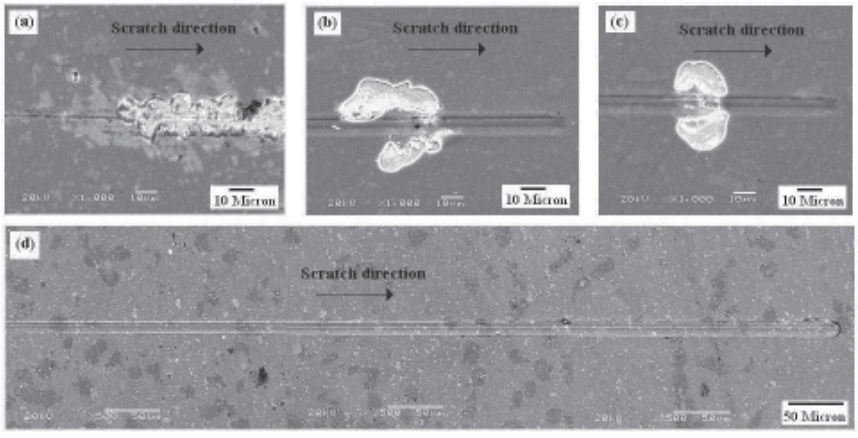

Figure 6. SEM images showing the scratch tracks and mode of failures of (a) sample 1, (b) sample 2, (c) sample 3 and (d) sample 5

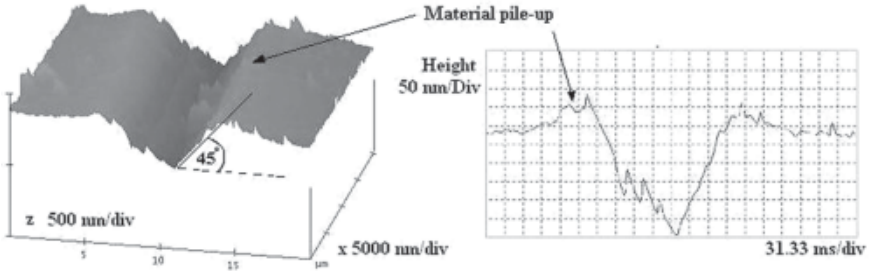

Figure 7. AFM images showing the orientation of the surface of the scratch track of deposited TiB_2 (sample 1)

of the coating. It thus indicates the tremendous improvement of the coating adhesion strength. In order to find the critical point of sample 5, the scratch distance was extended from 1,000 to 1,500 mm, and the experimental critical load of sample 5 was found to be 875.5 mN, almost 3 times that of sample 1.

Figure 7 shows the micro-scratch track of the TiB_2 coating examined under AFM of sample 1. It is obvious that there is a certain amount of material removal during a scratch test. AFM also reveals that the scratch track exhibits the formation of material pile-up along the sides. The pile-up was caused by plastic deformation of the coating, which was grooved by the indenter tip. In addition, the orientation of the surface of the scratch track is around 45 degrees, which is in line with the maximum shear stress direction. It is believed that contact with a hard, sharp indenter generates a stress field with large shear components.

Conclusions

1 Sputter-cleaning of the substrate helps to improve the TiB_2 coating hardness and adhesion strength.

2 The TiB_2 coatings produced with substrate bias possess low hardness, but good adhesion with the substrate. With biasing at the early stage of the whole deposition, the failure mode is changed from compressive spallation to wedge spallation, which obviously shows the improvement of the coating adhesion strength.

References

Berger, M., Coronel, E., and Olsson, E. (2004). Microstructure of d.c. magnetron sputter TiB_2 coatings. Surface and Coatings Technology, 185:240-244.

Berger, M., Karlsson, L., Larsson, M., and Hogmark, S. (2001). Low stress TiB_2 coatings with improved tribological properties. Thin Solid Films, 401: 179-186.

Cutler, A.R. (1991). Engineering Properties of Borides. Engineering Materials Handbook: Ceramic and Glasses. ASM International, p. 4.

Munro, G.R. (2000). Material properties of titanium diboride. Journal of Research of the National Institute of Standards and Technology, 105:709-720.

Oliver, C.W., and Pharr, M.G. (1992). An improved technique for determining hardness and elastic modulus using load and displacement sensing indentation experiments. Journal of Materials Research, 7:1,564-1,583.

Panich, N., and Sun, Y. (2005) Mechanical properties of TiB_2-based nano-structured coatings. Surface and Coatings Technology, (In press).

Xia, J., Li, X.C., Dong, H., and Bell, T. (2004). Nanoindentation and nanoscratch of thermal oxide layer on FeAl alloy. Journal of Materials Research, 19:291-300.